MOLECULAR AND CELLULAR BIOLOGY, Oct. 1993, p. 6346–6356
0270-7306/93/106346-11$02.00/0

Vol. 13, No. 10

The Yeast *KRE9* Gene Encodes an O Glycoprotein Involved in Cell Surface β-Glucan Assembly

JEFFREY L. BROWN AND HOWARD BUSSEY*

Biology Department, McGill University, 1205 Dr. Penfield Avenue, Montreal, Quebec, Canada H3A 1B1

Received 27 April 1993/Returned for modification 21 June 1993/Accepted 16 July 1993

The yeast *KRE9* gene encodes a 30-kDa secretory pathway protein involved in the synthesis of cell wall (1→6)-β-glucan. Disruption of *KRE9* leads to serious growth impairment and an altered cell wall containing less than 20% of the wild-type amount of (1→6)-β-glucan. Analysis of the glucan material remaining in a *kre9Δ* null mutant indicated a polymer with a reduced average molecular mass. *kre9Δ* null mutants also displayed several additional cell-wall-related phenotypes, including an aberrant multiply budded morphology, a mating defect, and a failure to form projections in the presence of α-factor. Double mutants were generated by crossing *kre9Δ* strains with strains harboring a null mutation in the *KRE1*, *KRE6*, or *KRE11* gene, and each of these double mutants was found to be inviable in the SEY6210 background. Similar crosses with null mutations in the *KRE5* and *SKN1* genes indicated that these double mutants were no more severely affected than *kre5Δ* or *kre9Δ* single mutants alone. Antibodies were generated against Kre9p and detected an O glycoprotein of approximately 55 to 60 kDa found in the extracellular medium of a strain overproducing Kre9p.

The yeast cell wall is an extracellular matrix of insoluble chitin, glycoproteins, and β-glucan polymers, cross-linked into a complex structural array at the cell surface. Fungal cell walls perform a number of essential roles in growth and morphogenesis (25), and *Saccharomyces cerevisiae* enables cell surface assembly to be studied at the genetic and biochemical levels. Although biochemical analyses have been useful in separating and characterizing the main structural components of the yeast extracellular matrix, identification of components involved in the biosynthesis of cell wall polymers has come predominantly from genetic approaches. The synthesis of chitin in *S. cerevisiae* is well understood, and a family of three homologous synthases are involved in assembly of the polymer. Disruption of the *CHS1* gene removes most of the chitin synthase activity in vitro (7); however, the product of the *CAL1* (*CHS3*) gene appears to be responsible for the synthesis of the majority of the chitin found in the cell wall periphery (36). *CHS2* has been shown to be required for the development of a proper septum between mother and daughter cells (35). Additional mutations have identified the *CSD3* and *CSD4* genes, which also appear to be required for chitin synthesis in vivo (6).

Mannoproteins represent a large fraction of the yeast cell wall, and many genes implicated in protein glycosylation have been identified and have provided insights into the stepwise synthesis of both O- and N-linked oligosaccharides (2, 15). The mannoprotein composition of the cell wall has also been studied biochemically, and several abundant glycoproteins that appear covalently cross-linked to extracellular matrix polysaccharides have been characterized (37), although their biological roles remain unclear.

The β-glucans are an additional class of abundant yeast cell surface polysaccharides, which represent approximately half of the total cell wall dry weight. In a simplified view, these glucans are composed of (1→3)-β-linked polymers averaging 1,500 residues in length and smaller, highly branched (1→6)-β-glucans with a degree of polymerization of approximately 150 to 200 residues. The cross-linked arrangement of these polysaccharides to each other and to chitin in the cell wall renders a large fraction of the glucan material insoluble in alkali, which has facilitated its isolation and structural analysis (12). The (1→3)-β- and (1→6)-β-linked cell wall glucans have classically been further subdivided on the basis of size, linkage composition, and solubility in alkali (20, 21), although the solubility in alkali of most of the total cell wall glucan in *cal1/chs3* mutants suggests that the conventional subclasses of glucan polymers may simply result from their differential cross-linking to chitin (30).

Whereas a number of components appear to be specifically involved in the assembly of extracellular matrix polysaccharides, genes that may be associated with the initiation or regulation of new cell wall growth have also been described. Mutations in the *PKC1*- and *BCK1* (*SLK1*)-encoded protein kinases display conditional lysis phenotypes which are suppressed by osmotic support (9, 19, 24). A large network of genes involved in cell morphogenesis including *SPA2*, the *BUD* and *BEM* genes, and a number of components of the cytoskeleton have been shown to be involved in initiating bud site selection and bud emergence (10), but how these components may also be involved in localizing the cell wall biosynthetic machinery to the site of a newly forming bud is not yet known.

Several genes involved in cell surface assembly have been identified through mutations that confer resistance to the K1 killer toxin protein, which kills sensitive yeast cells following binding to cell wall (1→6)-β-glucan. Thus, cells with mutations that disrupt the normal synthesis of the (1→6)-β-glucan receptor were identified by their ability to grow in the presence of toxin. The cloning and characterization of several killer resistance (*KRE*) genes have provided insight into the biosynthesis of this polymer. The earliest known step in the pathway for (1→6)-β-glucan assembly in yeast cells involves a luminal endoplasmic reticulum protein encoded by the *KRE5* gene. Cells harboring deletions of this locus fail to synthesize (1→6)-β-glucan, and they display severely impaired vegetative growth (22). Two genes, *KRE6*

* Corresponding author.

TABLE 1. Yeast strains used in this study

Strain	Genotype	Source or reference
SEY6210	*MATα leu2-3,112 ura3-52 his3-Δ200 lys2-801 trp1-Δ901 suc2-Δ9*	S. D. Emr
SEY6211	*MATa ade2-101 leu2-3,112 ura3-52 his3-Δ200 trp1-Δ901 suc2-Δ9*	S. D. Emr
HAB251-15B	SEY6210 autodiploid, *MATa/MATα leu2-3,112/leu2-3,112 ura3-52/ura3-52 his3-Δ200/his3-Δ200 lys2-801/lys2-801 trp1-Δ901/trp1-Δ901 suc2-Δ9/suc2-Δ9*	28
TA405	Autodiploid, *MATa/MATα his3/his3 leu2/leu2 can1/can1*	39
HAB522	*MATα kre9-1* in SEY6210	5
HAB556	*MATα kre9-4* in SEY6210	5
HAB635	*MATa kre1Δ::HIS3* in SEY6210	5
HAB751	*MATa kre9-1 ura3-52 leu2-3,112 his3-Δ200 trp1-Δ901 suc2-9Δ*	5
HAB806	*MATα kre11Δ::URA3* in SEY6210	5
HAB811	*MATα kre9Δ::HIS3* in TA405 haploid	This work
HAB812	*MATa kre9Δ::HIS3* in TA405 haploid	This work
HAB813	*MATα kre9Δ::HIS3* in SEY6210	This work
HAB814	*MATa kre9Δ::HIS3 ade2-101 leu2-3,112 ura3-52 his3-Δ200 trp1-Δ901 suc2-Δ9* generated from HAB813 backcrossed to SEY6211	This work
TR93	*MATa kre6Δ::HIS3* in SEY6210	29
TR178	*MATα skn1Δ::LEU2* in SEY6210	29
ML267	*MATα kre2Δ::TRP1* in SEY6210	M. Lussier
YDK5-3B	*MATa kre5Δ::HIS3* in TA405 haploid	22

and *SKN1*, that also appear to be involved in the early steps of (1→6)-β-glucan synthesis have been identified (28, 29). The predicted amino acid sequences of their products indicate two highly homologous integral membrane proteins with putative type II topology. Deletion of both *KRE6* and *SKN1* leads to a reduction in the cell wall (1→6)-β-glucan levels to 10% of those of isogenic wild-type strains. On the cytoplasmic side of the membrane, the product of the *KRE11* gene may act as a regulatory component of a membrane-associated (1→6)-β-glucan synthase complex (5). Disruption of *KRE11* leads to a 50% reduction in cell wall (1→6)-β-glucan levels. The product of the *KRE1* gene is probably plasma membrane associated through its hydrophobic C terminus, where it appears to be involved in a late stage of (1→6)-β-glucan assembly (3). Structural analysis of the glucan remaining in a *kre1Δ* mutant suggests a role for Kre1p in the addition of linear (1→6)-β-glucan side chains onto a core glucan backbone, allowing synthesis of the mature glucan polymer. Thus, an analysis of killer toxin-resistant mutants has identified genes in a pathway for (1→6)-β-glucan assembly, with products that are cytoplasmic, luminal, or membrane associated.

We have previously reported the isolation of strains with recessive *kre9* mutations and the mapping and cloning of the *KRE9* gene (5). The slow growth, killer resistance phenotype, and (1→6)-β-glucan reduction observed in mutants harboring the *kre9-1* or *kre9-4* alleles indicate defective cell surface assembly. Here we show that *KRE9* encodes a soluble secretory-pathway protein required for normal cell wall synthesis and growth. Antibodies specific for Kre9p identified an O-glycosylated protein, which, when overproduced, was detected extracellularly in the culture medium.

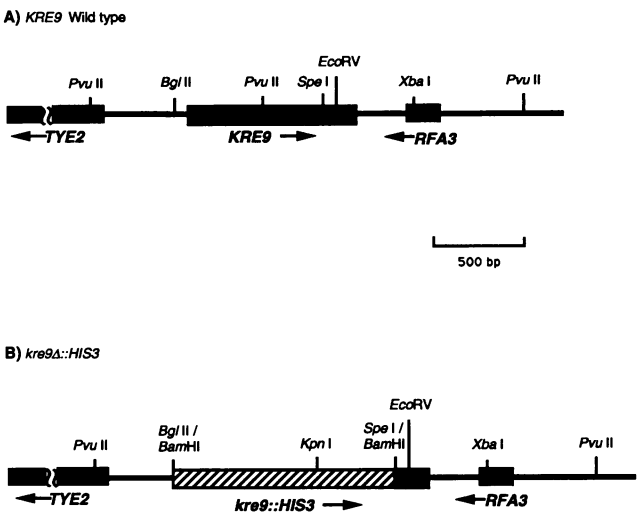

FIG. 1. Restriction map of the *KRE9* locus and schematic representation of the disruption construct. (A) Restriction map of the wild-type *KRE9* locus with respect to the adjacent open reading frames of the *TYE2(SWI3)* and *RFA3* genes. The solid boxes indicate the positions of the open reading frames, and arrows show the directions of transcription. (B) Schematic representation of the *kre9Δ::HIS3* deletion construct which replaces the N-terminal 230 amino acids of Kre9p encoded between the *Bgl*II and *Spe*I restriction sites with the complete *HIS3* gene.

MATERIALS AND METHODS

Yeast strains and procedures. The yeast strains used in this work are listed in Table 1. Cultures were grown under standard conditions as previously described (8). Routine transformations were carried out by the lithium acetate method (17), and yeast genetics and sporulation followed established procedures (34).

Plasmids and recombinant DNA techniques. Miniprep plasmids were purified from *Escherichia coli* MC1061 by the boiling method (32). Restriction endonucleases, Klenow and T4 DNA polymerases, and T4 DNA ligase were purchased from Bethesda Research Laboratories, Inc., Gaithersburg, Md.; Pharmacia LKB Biotechnology, Piscataway, N.J.; and New England BioLabs, Beverly, Mass., and were used as specified by the manufacturers.

Subcloning and sequencing *KRE9*. Series of nested deletions were generated for both strands of the *Bgl*II-*Xba*I region of *KRE9* (Fig. 1A) by using the Erase-a-Base System (Promega Corp., Madison, Wis.). Sequencing was carried out by the dideoxy method (33) with the Bluescript universal and reverse primers complementary to the pRS316 polylinker and synthetic oligonucleotides to specific regions of *KRE9*. The Sequenase Kit (U.S. Biochemicals, Cleveland, Ohio) was used for single-strand synthesis with [α-^{35}S]dATP as a substrate (Amersham Canada Limited, Oakville, Ontario, Canada). The complete sequence of *KRE9* (Fig. 2) was determined for both strands. The *KRE9* gene was also subcloned into the yeast multicopy vectors YEp351 and YEp352 as a 7-kb *Sma*I-*Sst*I fragment excised from the original pRS316-based genomic clone.

Disruption of *KRE9*. To generate a disruption of *KRE9*, an 821-bp *Bgl*II-*Spe*I fragment of the *KRE9* locus (Fig. 1A) was

```
-190                                                    AGATCTTCAAGGA
-177  TAATACAGGAATAGAACAGGAGTCTCAAAGCATTCTTGAAGCCAGATTTGCTCCAGTTT
-118  GATAGTTCCAAGAAGCGCTAAAAGTGGCAGTTCACACTTTGTTTTGATTACTAGGAATC
-59   TACTCTTTCGCTTTTTACTTCCTTCTCAGAGAATCAGCAACTGTGACATATTATAGATA
1     ATG CGT TTA CAA AGA AAT TCC ATC ATA TGT GCT TTG GTG TTT TTA
1      M  R  L  Q  R  N  S  I  I  C  A  L  V  F  L
46    GTC TCA TTT GTG CTG GGA GAT GTG AAT ATT GTT TCC CCC AGC TCC
16     V  S  F  V  L  G  D  V  N  I  V  S  P  S  S
91    AAG GCA ACA TTC AGT CCA AGT GGT GGT ACT GTC TCT GTT CCC GTT
31     K  A  T  F  S  P  S  G  G  T  V  S  V  P  V
136   GAA TGG ATG GAT AAT GGG GCA TAT CCC TCG TTA AGC AAG ATT TCA
46     E  W  M  D  N  G  A  Y  P  S  L  S  K  I  S
181   ACT TTC ACG TTC AGT CTT TGT ACT GGT CCT AAT AAC AAC ATT GAC
61     T  F  T  F  S  L  C  T  G  P  N  N  N  I  D
226   TGT GTG GCC GTA CTT GCC AGT AAA ATT ACT CCA AGT GAG CTA ACA
76     C  V  A  V  L  A  S  K  I  T  P  S  E  L  T
271   CAA GAT GAT AAA GTT TAC TCT TAC ACA GCT GAG TTT GCT TCG ACC
91     Q  D  D  K  V  Y  S  Y  T  A  E  F  A  S  T
316   TTA ACT GGG AAC GGT CAA TAT TAC ATT CAA GTT TTT GCC CAG GTG
106    L  T  G  N  G  Q  Y  Y  I  Q  V  F  A  Q  V
361   GAC GGT CAA GGT TAC ACT ATC CAT TAT ACA CCA AGA TTC CAG TTG
121    D  G  Q  G  Y  T  I  H  Y  T  P  R  F  Q  L
406   ACT TCC ATG GGC GGT GTT ACG GCT TAT ACA TAT AGT GCC ACA ACT
136    T  S  M  G  G  V  T  A  Y  T  Y  S  A  T  T
451   GAA CCT ACT CCC CAG ACT TCT ATT CAA ACA ACC ACT ACA AAC AAC
151    E  P  T  P  Q  T  S  I  Q  T  T  T  T  N  N
496   GCC CAA GCC ACT ACT ATT GAC AGT CGT TCA TTT ACT GTT CCG TAC
166    A  Q  A  T  T  I  D  S  R  S  F  T  V  P  Y
541   ACC AAG CAG ACT GGT ACG TCG CGT TTC GCT CCA ATG CAA ATG CAG
181    T  K  Q  T  G  T  S  R  F  A  P  M  Q  M  Q
586   CCA AAT ACT AAA GTG ACC GCT ACC ACA TGG ACA AGG AAA TTT GCC
196    P  N  T  K  V  T  A  T  T  W  T  R  K  F  A
631   ACT AGT GCT GTG ACA TAT TAC TCT ACC TTT GGG TCA TTG CCA GAG
211    T  S  A  V  T  Y  Y  S  T  F  G  S  L  P  E
676   CAA GCA ACT ACG ATA ACT CCT GGC TGG TCT TAT ACG ATA TCA TCG
226    Q  A  T  T  I  T  P  G  W  S  Y  T  I  S  S
721   GGA GTA AAC TAC GCT ACT CCT GCA TCT ATG CCT TCA GAT AAT GGT
241    G  V  N  Y  A  T  P  A  S  M  P  S  D  N  G
766   GGT TGG TAC AAA CCA TCC AAG AGA TTG TCT TTG TCT GCA AGG AAA
256    G  W  Y  K  P  S  K  R  L  S  L  S  A  R  K
811   ATC AAC ATG AGA AAA GTA TGA AAAATAGACGGCTTCTACTATCATCATTACA
271    I  N  M  R  K  V  STOP
863   GTAAGGGTTGAAGTCAGGAAAGGTTAAAAATAAAATAAATATCAAAAAGTTTTTAGCGG
922   AAGGCGTTAAGGCAGCAAGTACACATTCATTTATCTATCTATACATCTATAAACACAAC
981   TACAATTTTTTTTAGAAATGGAATTTATTATATGAAGGGAAGACATATAGAGGCAACAGT
1040  ACATAAAGGTAAGAATAAAAGCGATTTTAGCTAGTATATTTCTGGGTATTTCTTACATA
1099  GTCTCTGTAAAGCAACCACACCGTTTAAGCTTAAATCTTCGTTCTCCTTGAATTTGCAT
1158  AGTACAGCGTCTAGAATCAAAAATCCTAGCTCGCCGTCATCATTGTTCCTGCAAACAAA
1217  CTCATACCACGAGTCGATCTCAAATGTTTTATTCATAGATACACGAATATTGTTCAACG
1276  TAATCATTTCAACCTCGCTGCCGTTTTTCGATGATATGGTTGGCGATTGTAAAATCAAC
1335  TGAGATTCAGTGGGTTGTGATTTGATTTGCGCTATTATCCTAAACACAGGAGCATTGAC
1394  GTTGGAGATTTCTGTGGGGTCAACTCTTGGTGTTTCGCTGGCCATTTT
```

FIG. 2. Nucleotide and predicted amino acid sequences of *KRE9*. An 828-bp open reading frame is shown along with the predicted 276 amino acids of Kre9p. The positions of nucleotide sequences which correspond to the *Bgl*II (−190 to −185) and *Spe*I (631 to 636) restriction sites used for the *kre9*Δ::*HIS3* disruption construct (see Materials and Methods and Fig. 1B) are indicated in boldface type. A potential site for cleavage by signal peptidase would be after the G at amino acid residue 21 (38).

removed from a pRS316 plasmid containing a wild-type copy of the gene and the termini were rendered blunt with Klenow DNA polymerase. A 1.7-kb *Bam*HI fragment containing the complete *HIS3* gene was also treated with Klenow fragment and then blunt ligated into the vector to create *kre9*Δ::*HIS3*. A linear 3.6-kb *Pvu*II fragment containing the *HIS3* gene, flanked on either side by *KRE9* targeting sequences, was excised from this construct and used to disrupt the *KRE9* locus in strains HAB251-15B and TA405 by single-step gene replacement (31). Correct integrations were confirmed by genomic Southern blots (32).

(1→6)-β-glucan isolation, quantitation, and structural analysis. (1→6)-β-Glucan was isolated and quantified as previously described (3). Structural analysis was performed on glucan isolated from 2 liters of a wild-type TA405 culture or 5 liters of a HAB811 *kre9*Δ::*HIS3* culture, harvested in late-logarithmic phase. Gel filtration chromatography of glucans (~1 mg) was carried out on a Sepharose CL-6B (Pharmacia Fine Chemicals, Piscataway, N.J.) column (109 by 1 cm) with 0.1 M NaOH as the eluant, as described previously (5). Carbohydrate was measured as hexose by the borosulfuric acid method of Badin et al. (1). Proton-decoupled ^{13}C-nuclear magnetic resonance (^{13}C-NMR) spectra were generated for glucan samples as previously described (5) with a WH 400 spectrometer (Bruker Instruments, Billerica, Mass.) operated in the Fourier transform mode at 100.615 MHz with external dioxane at 67.4 ppm as a reference peak.

Electron microscopy. Exponentially growing wild-type and *kre9*Δ::*HIS3* cells were fixed for electron microscopy with 3% glutaraldehyde followed by 1% OsO_4, as described by Boone et al. (3). Sections were viewed on an EM410 electron microscope (Philips, Eindhoven, The Netherlands) operating at 80 kV.

Additional cell wall analyses. Cell wall chitin was observed by fluorescence with calcofluor white (30), and alcian blue binding was performed by the method of Friis and Ottolenghi (13). As a measure of cell wall integrity, stationary-phase cultures of wild-type or *kre9*Δ::*HIS3* cells were subjected to digestion with a (1→3)-β-glucanase preparation. Cultures were adjusted to a concentration of 10^7 cells per ml in 10 mM Tris-HCl (pH 7.5) and incubated in the presence of 100 μg of Zymolyase 100T (ICN Biochemicals, Cleveland, Ohio) per ml at 30°C with rotation. Aliquots were removed at 15-min intervals, and the optical density at 600 nm was measured. Glycogen levels in cell colonies were qualitatively assessed by using iodine vapors (11).

Quantitative mating and pheromone response. Wild-type and *kre9*-disrupted yeast strains were tested for their ability to conjugate by the procedure used by Raymond et al. (27), with strains SEY6210, SEY6211, HAB813, and HAB814. Matings were performed in triplicate by mixing approximately 10^7 cells from each of the appropriate strains in 1 ml of liquid yeast extract-peptone-dextrose (YEPD) and incubating the mixture for 3 h at 30°C. Serial dilutions were then plated onto YEPD to assess the total number of cells and onto yeast nitrogen base (YNB) selective media to determine the number of diploids present. The mating efficiency was calculated as the number of diploids capable of growth on selective media divided by the total number of cells on YEPD.

*MAT***a** haploid strains with disruptions at *kre9* were tested for their ability to respond to synthetic α-mating pheromone (Sigma, St. Louis, Mo.) Exponentially growing wild-type or *kre9*Δ::*HIS3* strains were incubated in the presence of α-factor at final concentrations of either 2 or 4 μg/ml in liquid YEPD at 30°C and were viewed by light microscopy.

Antibody production and purification. Polyclonal anti-Kre9p antibodies were generated in rabbits against a synthetic multiple-antigen peptide (Research Genetics, Huntsville, Ala.) with the sequence of the extreme C-terminal 15 amino acid residues of Kre9p (NH_2-KRLSLSARKINMR KV-COOH). Rabbits were initially injected with ~0.5 mg of the peptide in Freund's complete adjuvant, followed by five boosts with equivalent amounts of peptide in Freund's incomplete adjuvant at 2- to 3-week intervals. The Kre9p synthetic peptide (~1 mg) was coupled to cyanogen bromide-activated Sepharose CL-6B (Pharmacia) as specified by the manufacturer and used in a column with a total bed volume of 2 ml to affinity purify antiserum as described by Raymond et al. (26).

Western immunoblotting. Total-cell extracts were prepared from approximately 10^7 cells from exponentially growing cultures grown in YNB selective medium by lysis with glass beads. Membrane fractions were prepared from 50 ml of exponentially growing cultures by the method of Nakayama et al. (23) by centrifuging lysates at 10,000 × *g* for 20 min at 4°C (low-speed pellet) and at 100,000 × *g* for 1 h at 4°C (high-speed pellet). Extracellular proteins were concentrated from 100 ml of late-log-phase culture grown in YNB selective medium containing 5% (vol/vol) glycerol, using Amicon Centriprep-10 concentrators (W. R. Grace & Co., Danvers, Mass.). Protein samples were separated by sodium dodecyl sulfate-polyacrylamide gel electrophoresis by the method of Laemmli (18). After transfer to nitrocellulose, blots were incubated with affinity-purified anti-Kre9p antibodies diluted 1/500 and then with a horseradish peroxidase-coupled donkey anti-rabbit antibody (Amersham International, Amersham, United Kingdom) diluted 1/500 to 1/1,000 and developed with the 4-chloro-1-naphthol reagent.

Nucleotide sequence accession number. The DNA sequence in Fig. 2 has been deposited in GenBank under accession number L22517.

RESULTS

***KRE9* sequence and map position.** The *KRE9* gene was previously cloned and mapped to the left arm of chromosome X (5) (Fig. 1A). Sequencing of a *Bgl*II-*Xba*I region of *KRE9* revealed an open reading frame of 828 bp (Fig. 2) encoding a 30-kDa serine-plus-threonine rich protein of 276 amino acid residues. The hydrophobic N-terminal region of Kre9p resembles that of eukaryotic signal sequences, with a predicted cleavage site after amino acid 21 (38). A cluster of Lys and Arg residues (7 of 18) occurs at the extreme C terminus of the protein. No predicted sites for N-linked glycosylation exist, although the high proportion of serine and threonine residues (27%) offers many potential sites for O glycosylation. Searches with the predicted amino acid sequence of Kre9p failed to detect significant homology to proteins in the current GenBank and EMBL data bases.

We had previously mapped *KRE9* physically to λ clone 6699 in the library of mapped yeast genomic DNA fragments prepared by L. Riles and M. V. Olson (27a) and genetically to a position 19 cM from the *yur1* locus, in a region approximately 50 kb centromere-distal to *tif2* on the left arm of chromosome X (5). *KRE9* has also been independently sequenced by C. Loehning, C. Mueller, K. Freidel, and M. Ciriacy (GenBank accession number X56792) and identified as a small essential open reading frame (ORF831) juxtaposed between ORF369 and the *TYE2* (*SWI3*) gene. ORF369 is identical to the *RFA3* gene (GenBank accession number X59750), which was also found to hybridize to λ clone 6699 but had not been mapped further (4). Thus, the nucleotide sequence and mapping of the *KRE9* locus locates the *RFA3* and *TYE2* genes on the left arm of chromosome X (Fig. 1A).

Disruption of *KRE9*. A *kre9*Δ null mutation was generated by removing the N-terminal ATG start codon and 630 bp of the *KRE9* open reading frame from a wild-type copy of the gene and replacing it with a fragment containing *HIS3* (see Materials and Methods) (Fig. 1B). One of the chromosomal copies of *KRE9* was disrupted by single-step gene replacement in each of the diploid strains HAB251-15B and TA405. Integrations at the *KRE9* locus were confirmed for both these strains by genomic Southern hybridizations (Fig. 3). The resulting His^+ diploids were sporulated, and tetrads were dissected. *kre9*Δ::*HIS3* null mutants appeared as microcolonies after 8 to 10 days on YEPD at 30°C, as indicated by the 2:2 cosegregation of His^+ prototrophy, slow growth, and killer resistance for 50 tetrads examined. Thus, formally, *KRE9* is not an essential gene in these strains under these conditions. The *kre9*Δ::*HIS3* deletion removed 186 bp upstream of the predicted start codon of *KRE9*; however, this region does not appear to be required for *TYE2* expression. Subclones of *TYE2* beginning with the *Bgl*II restriction site used for the disruption (Fig. 1) fully complemented *tye2* mutations (8a).

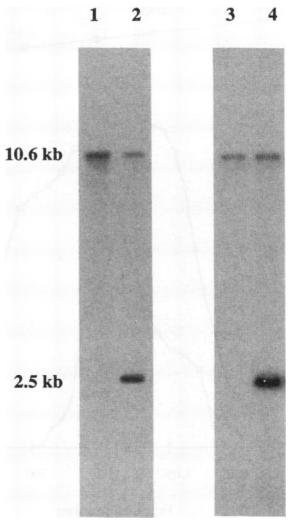

FIG. 3. Southern blot analysis of *kre9*Δ::*HIS3* disruptions. Total DNA isolated from parental diploid strains HAB251-15B (lane 1) and TA405 (lane 3) and strains HAB251-15B and TA405 heterozygous for the *kre9*Δ::*HIS3* deletion (lanes 2 and 4, respectively) was digested with *Kpn*I and probed with a labeled 1.3-kb *Xba*I-*Kpn*I fragment from the cloned *KRE9* gene (5). The presence of a *Kpn*I site in the *HIS3* gene at the *kre9*Δ locus is detected as a 2.5-kb fragment.

(1→6)-β-Glucan alterations. The slow growth, killer resistance, and glucan reduction previously found in *kre9-1* and *kre9-4* strains (5) strongly implicate the *KRE9* gene product in the synthesis of (1→6)-β-glucan. To establish that the more severe phenotype observed in *kre9*Δ::*HIS3* deletion mutants was also caused by a cell wall defect, we measured the levels of (1→3)-β- and (1→6)-β-glucan polymers from wild-type haploid strains and strains disrupted at the *kre9* locus. The total amount of alkali-insoluble (1→3)-β- plus (1→6)-β-glucan was not significantly different among the strains (Table 2); however, the levels of (1→6)-β-glucan

TABLE 2. Glucan levels in *kre9* mutants

Strain	*KRE* allele	(1→6)-β-Glucan (μg/mg [dry wt])[a]
SEY6210	Wild type	35.8 ± 0.8
HAB522	*kre9-1*	13.7 ± 2.6
HAB556	*kre9-4*	14.7 ± 0.6
HAB813	*kre9*Δ::*HIS3*	8.1 ± 1.1

[a] The (1→6)-β-glucan levels in *kre9* mutant strains and an isogenic wild-type parental strain were analyzed by the method of Boone et al. (3). Values for the *kre9-1* and *kre9-4* mutants were as previously described (5). Total alkali-insoluble glucan levels were not significantly different in any of these strains, with an average of 184 ± 20 μg/mg (dry weight). Error represents 1 standard deviation.

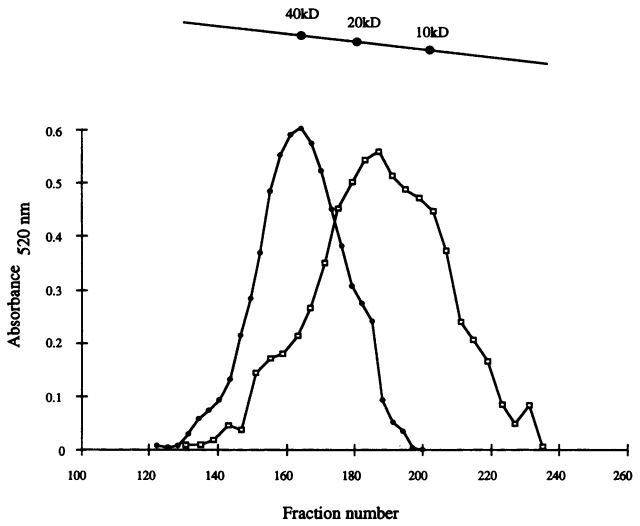

FIG. 4. Gel filtration chromatography of (1→6)-β-glucan purified from wild-type and *kre9*Δ::*HIS3* strains. The average molecular mass of (1→6)-β-glucan purified from either the wild-type strain (●) or the *kre9*Δ::*HIS3*-deleted strain HAB811 (□) was determined by using a Sepharose CL-6B column and known dextran standards. Approximately equal amounts of material (~1 mg) were loaded onto the column. Dextran blue eluted at fraction 94, indicating a column void volume of 30.5 ml.

were reduced in *kre9*Δ::*HIS3* mutants to 10 to 20% of the wild-type level (Table 2). These results suggest that *kre9* null mutations lead to a more severe growth and (1→6)-β-glucan alteration than the original alleles.

A large-scale purification of the residual (1→6)-β-glucan from a *kre9*Δ::*HIS3* mutant was performed to examine possible structural modifications to the (1→6)-β-glucan polymer. Gel filtration chromatography of the (1→6)-β-glucan isolated from the mutant strain indicated a polymer with an average molecular mass of 10 to 20 kDa, which is smaller than the ~40-kDa (1→6)-β-glucan isolated from a wild-type strain (Fig. 4). ^{13}C-NMR spectroscopy of the mutant glucan material also indicated a polymer that appeared structurally distinct from the wild type and probably contained an altered proportion of (1→3)-β- and (1→6)-β-linkages (Fig. 5B). Many of the resonance peaks from the spectrum could not be definitively assigned, although the polymer did appear to retain major signals characteristic of a (1→6)-β-linked glucan (Fig. 5A).

Additional cell wall analyses. *kre9*Δ::*HIS3* disrupted cells displayed an aberrant growth morphology and were often found as large, multiply budded aggregates that could not be separated by gentle agitation (Fig. 6B). To test whether the defect in *kre9*Δ::*HIS3* cells was specific to (1→6)-β-glucan or represented a pleiotropic effect on cell wall synthesis, we examined the other major cell wall components. Fluorescence staining with calcofluor white, a dye that preferentially binds cell wall chitin (30), appeared to be enhanced in *kre9*Δ::*HIS3* null mutants. Bud site selection in *kre9* null mutants was also examined by calcofluor staining of bud scars and appeared random, whereas isogenic parental cells showed a predominantly axial budding pattern (data not shown). Mutants stained normally with alcian blue, suggesting that glycosylation was not grossly altered by a *kre9* deletion. Staining with iodine indicated that *kre9*Δ::*HIS3* disrupted cells were glycogen positive. Electron micrographs of thin sections prepared from wild-type and *kre9*Δ::*HIS3* cells supported the biochemical evidence for a structural defect. Under the conditions used, *kre9*Δ mutants seem to have lost the laminar cell wall ultrastructure normally seen in wild-type cells (Fig. 6C and D).

Earlier studies had suggested that *kre9* mutant strains were more sensitive than the wild type to the (1→3)-β-glucanase-containing preparation Zymolyase, so the *kre9*Δ::*HIS3* null mutant was quantitatively assessed for susceptibility to Zymolyase lysis (see Materials and Methods). Stationary-phase cultures of HAB811 *kre9*Δ cells showed a ~50% reduction in optical density after incubation with 100 μg of Zymolyase 100T per ml for 15 min, whereas isogenic wild-type cells showed a modest (<5%) decrease.

Quantitative mass mating. Evidence of a *kre9*-related mating defect was first seen while backcrossing the original *kre9* mutants. Strains harboring the *kre9*Δ::*HIS3* null mutation were thus quantitatively assessed for their ability to conjugate. Wild-type strains SEY6210 and SEY6211 were found to mate at a frequency of $9 \times 10^{-3} \pm 1.4 \times 10^{-3}$ in liquid culture. Both HAB813 *MAT*α and HAB814 *MAT***a** strains harboring the *kre9*Δ::*HIS3* disruption were mated with the wild-type parental SEY6210 or SEY6211 strain, and they formed diploids at a frequency of $1 \times 10^{-3} \pm 5.6 \times 10^{-4}$. When the two *kre9* mutant strains were crossed to each other, diploids were formed at a frequency not significantly different from that of a *kre9*Δ strain crossed to a wild-type strain ($\sim 0.6 \times 10^{-3} \pm 0.3 \times 10^{-3}$). Thus, the approximately 10-fold reduction in mating efficiency with *kre9*Δ mutants was independent of cell type and was not cumulative when two *kre9*Δ mutants were crossed to each other.

Response to α-factor mating pheromone. *MAT***a** haploid *kre9*Δ cells were tested for their ability to shmoo in response to the α-mating pheromone. Exponentially growing wild-type and *kre9*Δ cells were incubated in the presence of α-factor at a final concentration of 2 μg/ml in liquid YEPD at 30°C. After 2 h, more than 75% of the wild-type cells had arrested as single cells or exhibited a characteristic shmoo morphology, while the *kre9*Δ cells remained as multiply budded aggregates with no obvious shmoo formation. Exposure to elevated levels of α-factor (4 μg/ml) for up to 4.5 h likewise produced no obvious morphological changes in the mutant cells (Fig. 7). The sensitivity of *kre9*Δ cells to pheromone-induced cell cycle arrest was tested by spotting ~1 μg of synthetic α-factor onto the surface of YEPD agar plates (pH 4.7) seeded with wild-type or *kre9*Δ cells. Both SEY6211 and HAB814 cells displayed a similar zone of growth inhibition of approximately 10 to 12 mm after 2 days at room temperature, suggesting that the G-protein-mediated signal transduction pathway is functional in *kre9*Δ cells. This apparent loss of the morphological response but retention of sensitivity to α-factor-induced cell cycle arrest may indicate that *kre9*Δ mutants are defective in their ability to effect polarized cell-wall growth.

Genetic interactions. The severity of the glucan reduction and growth impairment found in *kre9*Δ strains was consistent with the conclusion that Kre9p functions at an early step in (1→6)-β-glucan synthesis. To better understand the role of this gene in the pathway, we constructed double mutants with previously characterized *kre* mutations to look for potential genetic interactions.

Haploid strains HAB813 or HAB814, both carrying *kre9*Δ::*HIS3* mutations, were mated to isogenic strains of the opposite mating type harboring *kre1*Δ (HAB635), *kre6*Δ (TR93), *skn1*Δ (TR178), or *kre11*Δ (HAB806) deletions, and between 6 and 10 tetrads were dissected from each cross

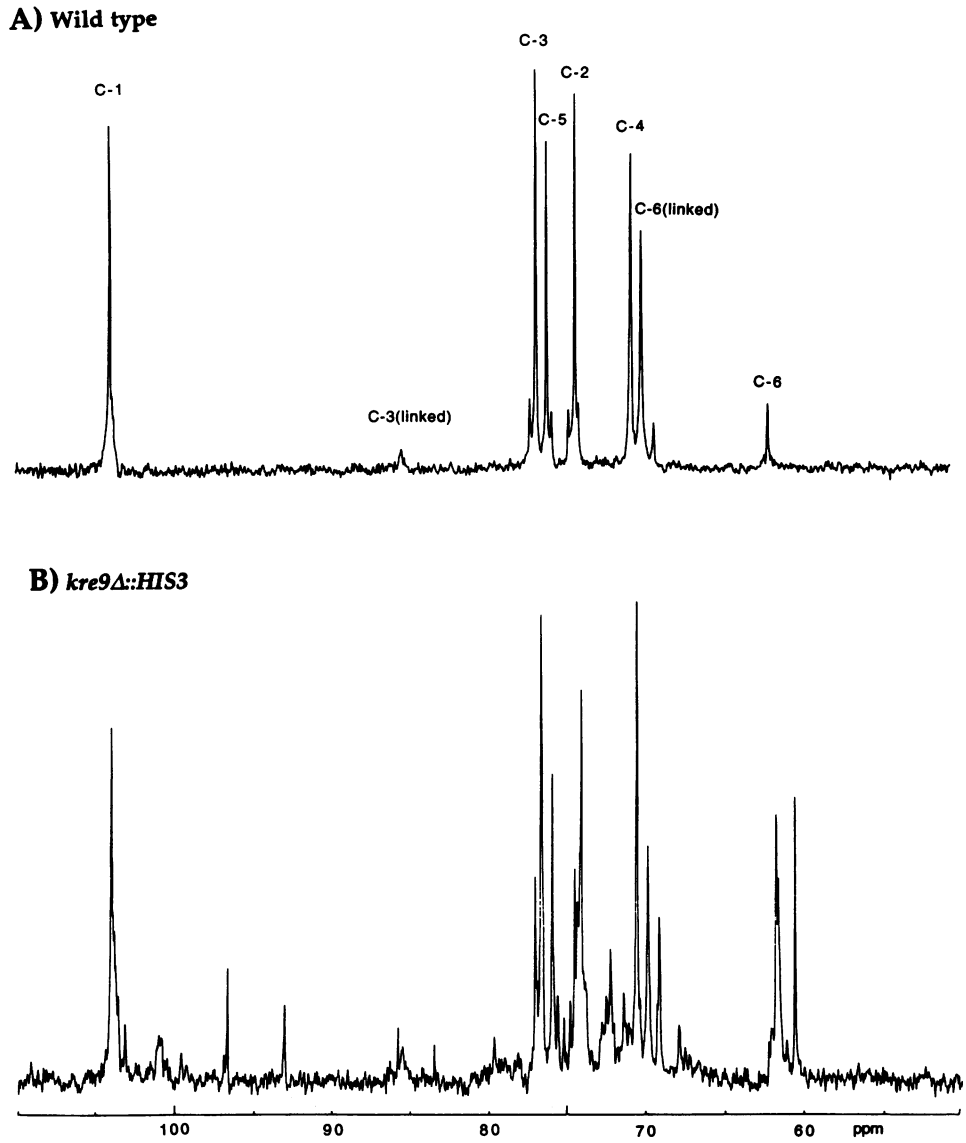

FIG. 5. ^{13}C-NMR spectra of (1→6)-β-glucan purified from wild-type and *kre9*Δ::*HIS3* strains. An assessment of the linkage composition of the residual (1→6)-β-glucan in the *kre9*Δ::*HIS3* strain HAB811 was determined by high-field ^{13}C-NMR spectroscopy (B). The predominant signals characteristic of wild-type (1→6)-β-glucan (A) have been labeled by using the assignments of Boone et al. (3).

onto YEPD medium. Segregants were scored for the selectable markers making the deletions, and double mutants were identified. The segregation patterns from *kre9*Δ crossed to *kre1*Δ [PD(0), NPD(1), TT(8)], *kre6*Δ [PD(1), NPD(1), TT(8)], and *kre11*Δ [PD(0), NPD(0), TT(6)] indicated that the double mutants were nonviable in all cases (PD indicates parental ditype, NPD indicates nonparental ditype, and TT indicates tetratype). The double-mutant spores were always found to have germinated, but they arrested with a similar terminal phenotype, as one to six large-budded cells. Double mutants isolated from the *kre9*Δ *skn1*Δ cross [PD(2), NPD(1), TT(7)] grew at rates comparable to those of the *kre9*Δ single mutants. The cell death observed in *kre9*Δ *kre1*Δ, *kre9*Δ *kre6*Δ, and *kre9*Δ *kre11*Δ double mutants indicates that these combinations of gene products are essential for the growth of SEY6210.

To assess potential genetic interactions with the *KRE5* gene, which defines the earliest known step in the pathway, we constructed a *kre5*Δ *kre9*Δ double mutant. It was necessary to generate a *kre5*Δ *kre9*Δ double heterozygous diploid in the TA405 background, because a *kre5*Δ::*HIS3* single mutation is lethal in SEY6210. Diploids generated by mating YDK5-3B to HAB811 were selected from YEPD medium and sporulated, and tetrads were dissected. Analysis of the segregation patterns from five four-spore tetrads [PD(2), NPD(0), TT(3)] indicated that the *kre5*Δ *kre9*Δ double mutants were viable in TA405 and grew slowly at rates equivalent to those of *kre5*Δ single mutants, suggesting that the double mutants were no more severely affected than *kre5*Δ single mutants.

Overproduction of *KRE9* was unable to suppress the slow growth or killer-resistant phenotypes associated with deletion of *kre1*Δ, *kre6*Δ, or *kre11*Δ. Multiple copies of *KRE1*,

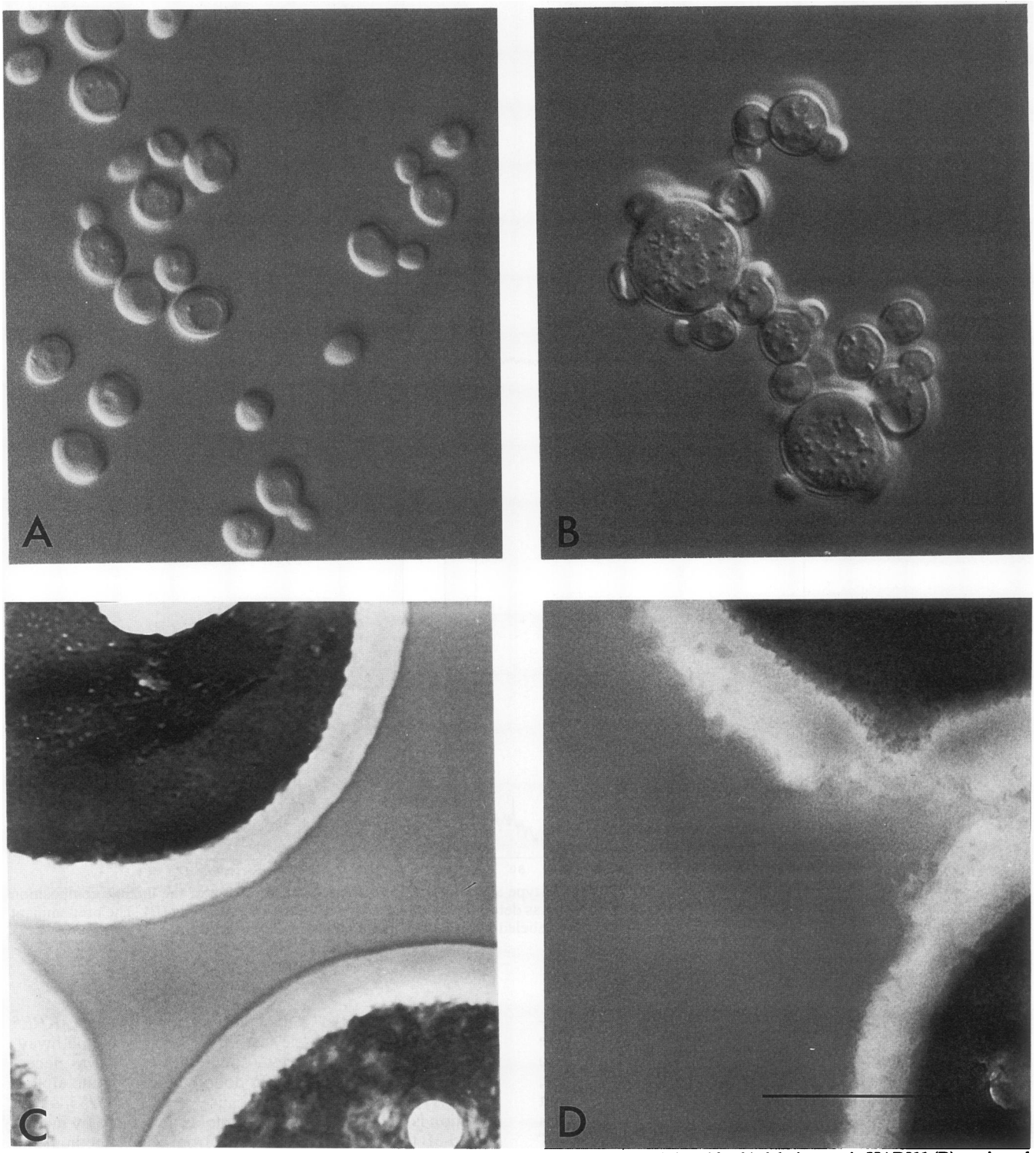

FIG. 6. Morphological effects of the *kre9*Δ::*HIS3* deletion. The wild-type *KRE9* strain (A) and *kre9*Δ deletion strain HAB811 (B) as viewed by Nomarski optics are shown. Electron micrographs of the cell walls of similar wild-type (C) and *kre9*Δ strains (D) are also shown. Exponentially growing cells were treated for microscopy as described in Materials and Methods. Bar, 1 μm.

KRE5, *KRE6*, *KRE11*, or *SKN1* also failed to suppress the loss of *KRE9*.

Kre9p is an O-linked glycoprotein. To identify the *KRE9* gene product, we generated an affinity-purified Kre9p antiserum (see Materials and Methods). Whole-cell extracts, membrane preparations, and concentrated extracellular media from a strain overexpressing the *KRE9* gene on a multicopy plasmid and from a *kre9*Δ strain were probed with

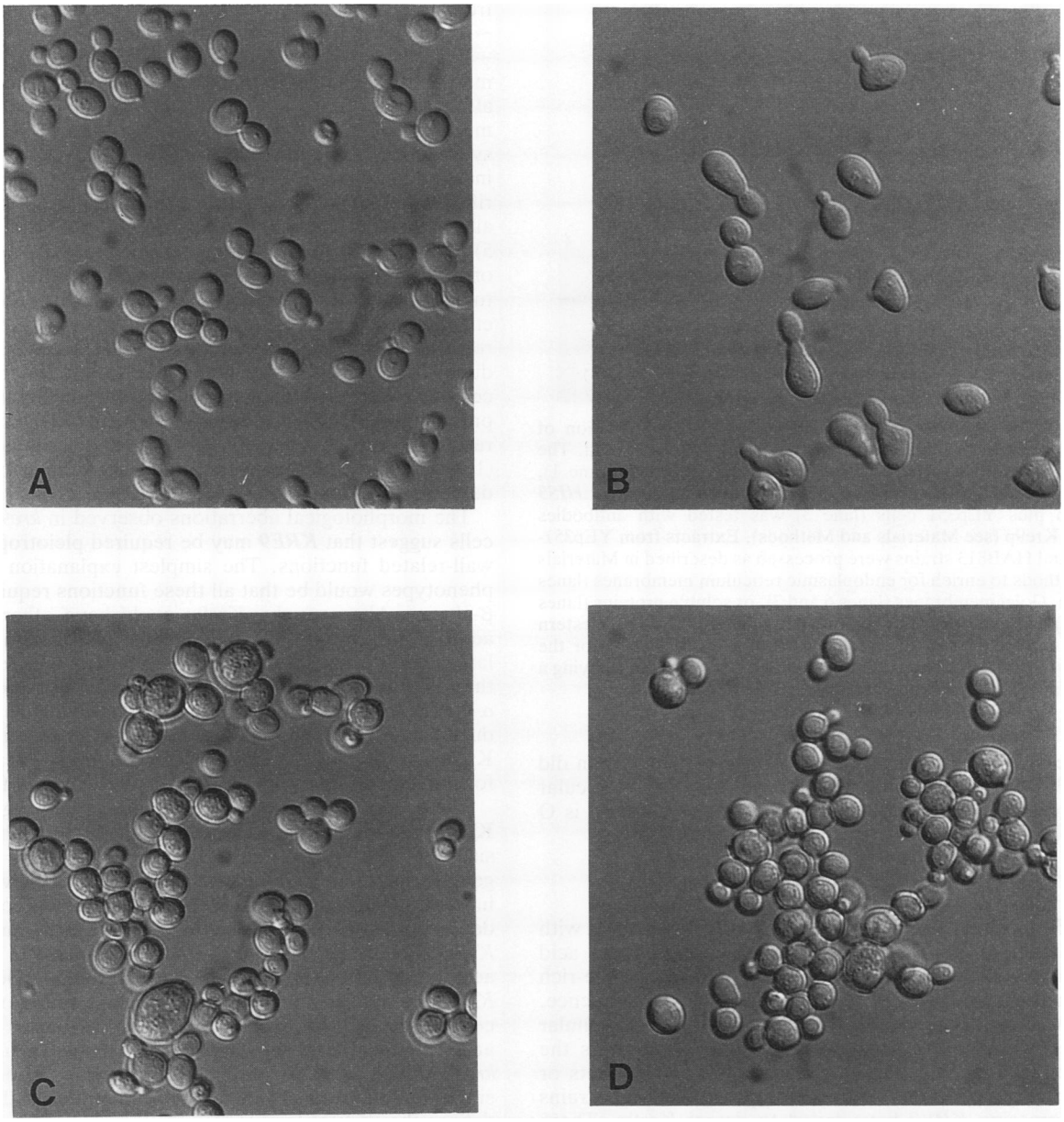

FIG. 7. Response to the α-factor pheromone. Exponentially growing wild-type SEY6211 cells and strain HAB814 *kre9*Δ cells were tested for their ability to shmoo on exposure to the α-mating pheromone. SEY6211 (A and B) and HAB814 (C and D) cells were incubated in the presence of either H_2O (A and C) or synthetic α-factor at 4 μg/ml (B and D) and photographed after 2.5 h.

the affinity-purified antiserum for the presence of Kre9p by a Western blot procedure. Figure 8A shows a major immunoreactive protein band of approximately 55 to 60 kDa in the extracellular medium from the strain overproducing Kre9p (lane 1). No signal was detected in the extracellular medium from the wild-type strain SEY6210 (lane 2) or the *kre9*Δ deletion mutant (lane 3). Kre9p was also undetectable in cell wall preparations and various fractions derived from cell lysates from each of these strains (Fig. 8A and data not shown).

The apparent molecular mass of the 55- to 60-kDa band recognized in Fig. 8A, lane 1, was significantly larger than that expected from the predicted protein sequence of Kre9p (30 kDa). No N-linked glycosylation sites occur in the predicted sequence, but the abundance of serine and threonine residues, the heterogeneous size of the protein, and the extracellular location of the protein when overproduced suggested that Kre9p may be O glycosylated. To test this possibility, we overexpressed *KRE9* in a strain harboring a deletion at the *KRE2* locus. *KRE2* (*MNT1*) encodes an (1→2)-α-mannosyltransferase, which when deleted limits O-linked chains to two mannose residues (14, 16). Western blots on the extracellular medium from either SEY6210 or *kre2*Δ::*TRP1* strains transformed with a multicopy YEp351-*KRE9* plasmid were probed with the affinity-purified Kre9p antibody (Fig. 8B). Kre9p isolated from the

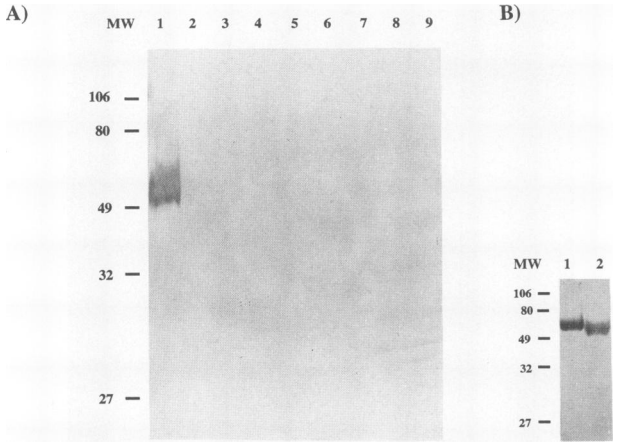

FIG. 8. Western blot analysis of Kre9p. (A) Identification of Kre9p from yeast strains carrying a multicopy *KRE9* plasmid. The extracellular medium from SEY6210 plus YEp351-*KRE9* (lane 1), SEY6210 plus YEp351 (lane 2), or HAB813 harboring a *kre9*Δ::*HIS3* deletion plus YEp351 cells (lane 3) was tested with antibodies against Kre9p (see Materials and Methods). Extracts from YEp351-*KRE9* and HAB813 strains were processed as described in Materials and Methods to enrich for endoplasmic reticulum membranes (lanes 4 and 5), Golgi membranes (lanes 6 and 7), or soluble proteins (lanes 8 and 9) and were probed with anti-Kre9p antibodies. (B) Western blot of extracellular medium from either SEY6210 (lane 1) or the *kre2*(*mnt1*)Δ::*TRP1* disrupted strain ML267 (lane 2), both carrying a multicopy YEp351-*KRE9* plasmid.

*kre2*Δ::*TRP1* strain (lane 2) migrated more quickly than did the wild-type Kre9p (lane 1), with an apparent molecular mass of approximately 50 kDa, indicating that Kre9p is O glycosylated.

DISCUSSION

KRE9 appears to encode a secretory pathway protein with a predicted molecular mass of 30 kDa. The amino acid sequence of Kre9p indicates a serine-plus-threonine-rich protein with an apparent amino-terminal signal sequence. When overproduced, Kre9p was found in the extracellular culture medium, directly demonstrating that it enters the secretory pathway. Western blots on total-cell extracts or membrane preparations from wild-type strains and strains overexpressing *KRE9* have failed to detect Kre9p. These results are consistent with a low wild-type level of the protein in a luminal or periplasmic compartment, but the actual cellular location of Kre9p has not been determined.

Overexpressing *KRE9* in a strain deleted for the *KRE2*/*MNT1*-encoded (1→2)-α-mannosyltransferase provided direct evidence for O mannosylation. The 55- to 60-kDa Kre9p band from a wild-type strain shifted in molecular mass to approximately 50 kDa in a *kre2*Δ background. The heterogeneous size distribution of Kre9p is retained in the *kre2*Δ mutant strain, arguing that the heterogeneity is independent of O-mannose chain length. Other sources of heterogeneity may be variation in O glycosylation sites or additional posttranslational modifications.

Disruption of *KRE9* leads to a cell wall defect and a major reduction (80 to 90%) in the amount of cell wall (1→6)-β-glucan. Cells harboring the *kre9*Δ mutation are Zymolyase sensitive and extremely slow growing and produce a remnant (1→6)-β-linked polymer that appears altered in structure and size. Size analysis of the residual (1→6)-β-glucan from a *kre9*Δ mutant indicates an average molecular mass of ~10 to 20 kDa, which is significantly smaller than the ~40-kDa wild-type material. A shift in the average molecular mass of the (1→6)-β-glucan is also seen in *kre1*Δ mutants (3), although the more severe phenotype observed in *kre9*Δ mutants suggests that Kre9p is affecting (1→6)-β-glucan synthesis in a different manner. ^{13}C-NMR spectroscopy also indicated structural modifications in the (1→6)-β-glucan purified from a *kre9*Δ mutant, which displayed potentially altered linkage ratios in comparison with the wild type (Fig. 5). Prominent structural changes associated with the deletion of *KRE9* are the increased proportion of residues unsubstituted at C-6 (61.5 ppm) and the appearance of the α and β enantiomeric forms of unsubstituted C-1 (97 and 93.5 ppm, respectively), consistent with a (1→6)-β-linked polymer reduced in size. Unlike the mutant glucan purified from *kre1*Δ cells, the *kre9*Δ polymer had no significant increase in the proportion of C-3-linked residues (85 ppm). Together, these results indicate that deletion of *KRE9* affects synthesis of the (1→6)-β-glucan in a manner distinct from that produced by deletion of *KRE1*.

The morphological aberrations observed in *kre9*Δ mutant cells suggest that *KRE9* may be required pleiotropically for wall-related functions. The simplest explanation for these phenotypes would be that all these functions require (1→6)-β-glucan. Alternatively, Kre9p could have other roles, in addition to (1→6)-β-glucan synthesis. Null mutants formed large, multiply budded structures, which were defective in their ability to form projections in the presence of the α-mating pheromone. *kre9*Δ mutants also displayed a reduced mating efficiency and a random budding pattern. Thus Kre9p, or the presence of (1→6)-β-glucan, may be necessary for implementing normal polarized cell wall growth.

The severity of the *kre9*Δ glucan phenotype suggests that Kre9p may be involved early in (1→6)-β-glucan biosynthesis. To identify possible epistasis relationships or other genetic interactions between components believed to be involved in the synthesis of the polymer, we constructed double mutants by using deletion mutants with mutations of *KRE9*, *KRE1*, *KRE5*, *KRE6*, *KRE11*, and *SKN1*. The interactions observed are summarized in Fig. 9. Deletion of *KRE9* in strains harboring a *kre5* null mutation, which completely lack alkali-insoluble (1→6)-β-glucan, indicated an epistatic relationship between these two genes. *kre9*Δ *kre5*Δ double mutants grew no more slowly than did *kre5*Δ single mutants, consistent with the hypothesis that *KRE5* defines the earliest known step in the pathway.

Another cross suggested that the *kre9*Δ and *kre11*Δ mutations interact and that, together, Kre9p and Kre11p are essential for growth in the SEY6210 background. KRE11 is predicted to encode a cytoplasmic possible regulatory protein, involved in synthesis of the (1→6)-β-glucan polymer (5). Similarly, *kre11*Δ *kre6*Δ double mutants have previously been shown to be nonviable (5, 29). The *KRE6* and *SKN1* genes encode highly homologous type II transmembrane proteins, which together are required for (1→6)-β-glucan synthesis. The cytoplasmic and luminal domains of these proteins could be involved, perhaps in complexes, with other proteins affecting the synthesis of this polymer. Although the lethality of *kre11*Δ *kre6*Δ, *kre6*Δ *kre9*Δ, and *kre9*Δ *kre11*Δ double mutations may be consistent with such a model, it remains possible that these interactions are indirect. Nevertheless, genes with cytoplasmic, luminal, or membrane-associated products have been identified which individually affect (1→6)-β-glucan synthesis and which interact genetically. The finding that *kre9*Δ *skn1*Δ double mutants

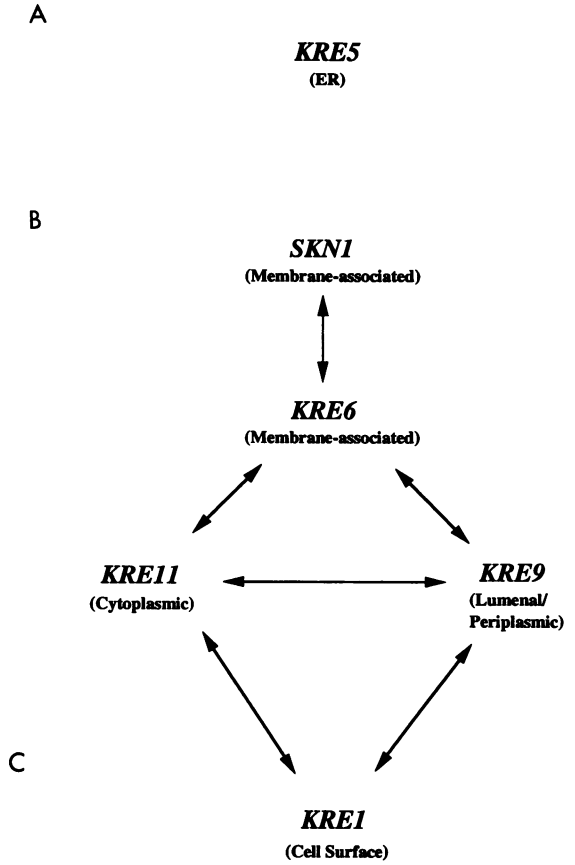

FIG. 9. Model depicting interactions between genes involved in the assembly of (1→6)-β-glucan. Arrows show genetic interactions in which double mutants are more severely affected than the individual single mutants, and the putative locations of the gene products are indicated. (A) *KRE5* appears epistatic to the other known genes and is shown at the earliest step in the pathway. (B) The homologous *KRE6* and *SKN1* genes also appear to be involved early in (1→6)-β-glucan synthesis, and together these gene products are necessary for growth in SEY6210. Disruption of *KRE11* is lethal in combination with mutations in *KRE6*, and *KRE11* has also been shown to interact genetically with *KRE1*. *KRE9* also appears essential for the growth of strains with null mutations in *KRE6*, *KRE11*, or *KRE1*. (C) *KRE1* is positioned late in the model, since its product appears to be involved in the completion of (1→6)-β-glucan synthesis. ER, endoplasmic reticulum.

grew as well as *kre9*Δ single mutants may be explained if *KRE9* were epistatic to *SKN1* or if Skn1p required Kre9p to function. The presence of Kre6p, a functionally redundant and potentially more prominent biosynthetic homolog of Skn1p, may also provide sufficient (1→6)-β-glucan synthesis for the growth of *kre9*Δ *skn1*Δ double mutants (29).

The *kre9*Δ *kre1*Δ double mutants were also nonviable. Kre1p is believed to be necessary for the addition of (1→6)-β-glucan side chains to a core glucan backbone. The more severe phenotype seen in the *kre9*Δ *kre1*Δ double mutants implies that Kre1p can function on the residual polymer made in a *kre9*Δ mutant. The ^{13}C-NMR spectrum of the *kre9*Δ mutant glucan, discussed above, may support this notion. Thus, a simple explanation of the nonviability of *kre9*Δ *kre1*Δ double mutants would be a cumulative reduction in the levels of the polymer to less than that required for viability of this strain.

In summary, the initial characterization of the *KRE9* gene and its product suggests an important role for Kre9p in β-glucan biosynthesis. The availability of anti-Kre9p antibodies and the ability to produce Kre9p extracellularly provide tools to examine biochemically the function of this protein.

ACKNOWLEDGMENTS

We thank the members of the Bussey laboratory for helpful discussions, the Image Centre for photographic expertise, Kathy Hewitt for electron microscopy, and Silvi Bilodeau and Arthur Perlin for ^{13}C-NMR spectroscopy.

This research was supported by Operating and Biotechnology Strategic Grants from The Natural Sciences and Engineering Research Council of Canada.

REFERENCES

1. **Badin, J., C. Jackson, and M. Schubert.** 1953. Improved method for determination of plasma polysaccharides with tryptophan. Proc. Soc. Exp. Biol. Med. **84**:228–291.
2. **Ballou, C. E.** 1982. Yeast cell wall and cell surface, p. 335–357. *In* J. N. Strathern, E. W. Jones, and J. R. Broach (ed.), The molecular biology of the yeast *Saccharomyces*: metabolism and gene expression. Cold Spring Harbor Laboratory, Cold Spring Harbor, N.Y.
3. **Boone, C., S. S. Sommer, A. Hensel, and H. Bussey.** 1990. Yeast *KRE* genes provide evidence for a pathway of cell wall β-glucan assembly. J. Cell Biol. **110**:1833–1843.
4. **Brill, S. J., and B. Stillman.** 1991. Replication factor-A from *Saccharomyces cerevisiae* is encoded by three essential genes coordinately expressed at S phase. Genes Dev. **5**:1589–1600.
5. **Brown, J. L., Z. Kossaczka, B. Jiang, and H. Bussey.** 1993. A mutational analysis of killer toxin resistance in *Saccharomyces cerevisiae* identifies new genes involved in cell wall (1→6)-β-glucan synthesis. Genetics **133**:837–849.
6. **Bulawa, C. E.** 1992. *CSD2*, *CSD3*, and *CSD4* genes required for chitin synthesis in *Saccharomyces cerevisiae*: the *CSD2* gene product is related to chitin synthases and to developmentally regulated proteins in *Rhizobium* species and *Xenopus laevis*. Mol. Cell. Biol. **12**:1764–1776.
7. **Bulawa, C. E., M. L. Slater, E. Cabib, J. Au-Young, A. Sburlati, W. L. Adair, and P. W. Robbins.** 1986. The *S. cerevisiae* structural gene for chitin synthase is not required for chitin synthesis *in vivo*. Cell **46**:213–225.
8. **Bussey, H., W. Sacks, D. Galley, and D. Saville.** 1982. Yeast killer plasmid mutations affecting toxin secretion and activity and toxin immunity function. Mol. Cell. Biol. **2**:346–354.

8a. **Ciriacy, M.** Personal communication.

9. **Costigan, C., S. Gehrung, and M. Snyder.** 1992. A synthetic lethal screen identifies *SLK1*, a novel protein kinase homolog implicated in yeast cell morphogenesis and cell growth. Mol. Cell. Biol. **12**:1162–1178.
10. **Drubin, D. G.** 1991. Development of cell polarity in budding yeast. Cell **65**:1093–1096.
11. **Farkas, I., T. A. Hardy, M. G. Goebl, and P. J. Roach.** 1991. Two glycogen synthase isoforms in *Saccharomyces cerevisiae* are coded by distinct genes that are differentially controlled. J. Biol. Chem. **266**:15602–15607.
12. **Fleet, G. H., and D. J. Manners.** 1976. Isolation and composition of an alkali-soluble glucan from the cell walls of *Saccharomyces cerevisiae*. J. Gen. Microbiol. **94**:180–192.
13. **Friis, J., and P. Ottolenghi.** 1970. The genetically determined binding of alcian blue by a minor fraction of yeast cell walls. C.R. Trav. Lab. Carlsberg **37**:327–341.
14. **Häusler, A., L. Ballou, C. E. Ballou, and P. W. Robbins.** 1992. Yeast glycoprotein biosynthesis: *MNT1* encodes an α-1,2-mannosyltransferase involved in O-glycosylation. Proc. Natl. Acad. Sci. USA **89**:6846–6850.
15. **Herscovics, A., and P. Orlean.** 1993. Glycoprotein biosynthesis in yeast. FASEB J. **7**:540–550.

16. **Hill, K., C. Boone, M. Goebl, R. Puccia, A. M. Sdicu, and H. Bussey.** 1992. Yeast *KRE2* defines a new gene family encoding probable secretory proteins, and is required for the correct *N*-glycosylation of proteins. Genetics **130:**273–283.
17. **Ito, H., M. Fukuda, M. Murata, and A. Kimura.** 1983. Transformation of intact yeast cells with alkali cations. J. Bacteriol. **153:**163–168.
18. **Laemmli, U. K.** 1970. Cleavage of structural proteins during the assembly of the head of bacteriophage T4. Nature (London) **227:**680–685.
19. **Lee, K. S., and D. E. Levin.** 1992. Dominant mutations in a gene encoding a putative protein kinase (*BCK1*) bypass the requirement for a *Saccharomyces cerevisiae* protein kinase C homolog. Mol. Cell. Biol. **12:**172–182.
20. **Manners, D. J., A. J. Masson, and J. C. Patterson.** 1973. The structure of a β-(1→3)-D-glucan from yeast cell walls. Biochem. J. **135:**19–30.
21. **Manners, D. J., A. J. Masson, and J. C. Patterson.** 1973. The structure of a β-(1→6)-D-glucan from yeast cell walls. Biochem. J. **135:**31–36.
22. **Meaden, P., K. Hill, J. Wagner, D. Slipetz, S. S. Sommer, and H. Bussey.** 1990. The yeast *KRE5* gene encodes a probable endoplasmic reticulum protein required for (1→6)-β-D-glucan synthesis and normal cell growth. Mol. Cell. Biol. **10:**3013–3019.
23. **Nakayama, K., T. Nagasu, Y. Shimma, J. Kuromitsu, and Y. Jigami.** 1992. *OCH1* encodes a novel membrane bound mannosyltransferase: outer chain elongation of asparagine-linked oligosaccharides. EMBO J. **11:**2511–2519.
24. **Paravicini, G., M. Cooper, L. Friedli, D. J. Smith, J. L. Carpentier, L. S. Klig, and M. A. Payton.** 1992. The osmotic integrity of the yeast cell requires a functional *PKC1* gene product. Mol. Cell. Biol. **12:**4896–4905.
25. **Peberdy, J. F.** 1989. Fungal cell walls-a review, p. 5–30. *In* P. J. Kuhn, A. P. J. Trinci, M. J. Jung, M. W. Goosey, and L. G. Coppings (ed.), Biochemistry of cell walls and membranes in fungi. Springer-Verlag KG, Berlin.
26. **Raymond, C. K., P. J. O'Hara, G. Eichinger, J. H. Rothman, and T. H. Stevens.** 1990. Molecular analysis of the yeast *VPS3* gene and the role of its product in vacuolar protein sorting and vacuolar segregation during the cell cycle. J. Cell Biol. **111:**877–892.
27. **Raymond, M., P. Gros, M. Whiteway, and D. Thomas.** 1992. Functional complementation of yeast *ste6* by a mammalian multidrug resistance *mdr* gene. Science **256:**232–234.
27a. **Riles, L., and M. V. Olson.** Personal communication.
28. **Roemer, T., and H. Bussey.** 1991. Yeast β-glucan synthesis: *KRE6* encodes a predicted type II membrane protein required for glucan synthesis in vivo and for glucan synthase activity in vitro. Proc. Natl. Acad. Sci. USA **88:**11295–11299.
29. **Roemer, T., S. Delaney, and H. Bussey.** 1993. *SKN1* and *KRE6* define a pair of functional homologs encoding putative membrane proteins involved in β-glucan synthesis. Mol. Cell. Biol. **13:**4039–4048.
30. **Roncero, C., M. H. Valdivieso, J. C. Ribas, and A. Duran.** 1988. Isolation and characterization of *Saccharomyces cerevisiae* mutants resistant to calcofluor white. J. Bacteriol. **170:**1950–1954.
31. **Rothstein, R. J.** 1983. One step gene-disruption in yeast. Methods Enzymol. **101:**202–211.
32. **Sambrook, J., E. F. Fritsch, and T. Maniatis.** 1989. Molecular cloning: a laboratory manual, 2nd ed. Cold Spring Harbor Laboratory, Cold Spring Harbor, N.Y.
33. **Sanger, F., S. Nicklen, and A. R. Coulson.** 1977. DNA sequencing with chain-terminating inhibitors. Proc. Natl. Acad. Sci. USA **74:**5463–5467.
34. **Sherman, F., G. R. Fink, and J. B. Hicks.** 1986. Methods in yeast genetics. Cold Spring Harbor Laboratory, Cold Spring Harbor, N.Y.
35. **Silverman, S. J., A. Sburlati, M. L. Slater, and E. Cabib.** 1988. Chitin synthase 2 is essential for septum formation and cell division in *Saccharomyces cerevisiae*. Proc. Natl. Acad. Sci. USA **85:**4735–4739.
36. **Valdivieso, M. H., P. C. Mol, J. A. Shaw, E. Cabib, and A. Duran.** 1991. *CAL1*, a gene required for activity of chitin synthase 3 in *Saccharomyces cerevisiae*. J. Cell Biol. **114:**101–109.
37. **van Rinsum, J., F. M. Klis, and H. van den Ende.** 1991. Cell wall glucomannoproteins of *Saccharomyces cerevisiae mnn9*. Yeast **7:**717–726.
38. **von Heijne, G.** 1984. How signal sequences maintain cleavage specificity. J. Mol. Biol. **173:**243–251.
39. **Whiteway, M., and J. W. Szostak.** 1985. The *ARD1* gene of yeast functions in the switch between the mitotic cell cycle and alternative developmental pathways. Cell **43:**483–492.